NÖRO PSİKİYATRİ ARŞİVİ
ARCHIVES OF NEUROPSYCHIATRY

RESEARCH ARTICLE

Article No: 84

Arch Neuropsychiatry 2026;63:535–540
https://doi.org/10.29399/npa.29228

Subcortical Shape Alterations in Schizophrenia: A Single-Site Validation of ENIGMA's Meta-Analytic Findings

Sıla ÖZKAL[1]*, Begüm TAHHAN[1]*, Çağan KAPLAN[1]*, Yıldırım ADALIOĞLU[1]*, Aslı Ceren HINÇ[2], Furkan YAZICI[3], Yiğit ERDOĞAN[3], Ali Saffet GÖNÜL[3]

[1]Medical Student, Ege University School of Medicine, Bornova, Izmir, Türkiye
[2]Department of Psychiatry, Izmir City Hospital, Izmir, Türkiye
[3]SoCAT Lab Department of Psychiatry, School of Medicine Ege University, Izmir, Türkiye

ABSTRACT

Introduction: Although meta-analysis by combining samples from multiple studies increases the statistical power, differences in study designs, participant characteristics, and outcome measures can create heterogeneity. Therefore, it might be helpful to validate the results of meta-analysis in independent smaller single site samples. This study investigates the shape characteristics of subcortical structures in schizophrenia patients by replicating and extending findings from a large multi-site meta-analysis using a single-site cohort.

Methods: Employing the ENIGMA shape analysis protocol, we examined the MRI images of 57 patients and 37 controls using FreeSurfer.

Results: Compared with controls, schizophrenia was associated with surface contraction in the left hippocampus, bilateral thalamus, bilateral nucleus accumbens, and right amygdala, alongside surface expansion in the bilateral putamen, left caudate, and bilateral pallidum; the right caudate showed both expansion and contraction. Thickness reductions were observed in the bilateral hippocampus, bilateral thalamus, bilateral accumbens, and right amygdala, while thickening was most evident in the right pallidum; the caudate, putamen, and left pallidum showed bidirectional thickness patterns. Antipsychotic dosage showed no significant effect on shape measures. Notably, our effect sizes surpassed those observed in earlier multi-site work. Larger effect sizes observed in our study could be attributed to the higher sampling variability due to relatively smaller sample size or increased clinical severity among patients from our single center compared to the patient populations in the meta-analysis.

Conclusions: Overall, these findings underscore the utility of shape-based analyses for understanding schizophrenia neuroanatomy, emphasize considering the clinical characteristics of the study sample, and highlight the importance of single-site validation—particularly for cohorts not represented in larger consortia that have higher baseline clinical severity.

Keywords: Antipsychotic, neuroimaging, schizophrenia, shape analysis, subcortical structures

Cite this article as: Özkal S, Tahhan B, Kaplan Ç, Adalıoğlu Y, Hınç AC, Yazıcı F et al. Subcortical Shape Alterations in Schizophrenia: A Single-Site Validation of ENIGMA's Meta-Analytic Findings. Arch Neuropsychiatry 2026;63:535–540. doi: 10.29399/npa.29228

INTRODUCTION

Schizophrenia is generally a chronic and debilitating mental disorder that affects approximately 1 in 100 individuals worldwide (1). It is characterized by cognitive impairments, emotional aberrations, and behavioral anomalies, which undermine basic processes of perception, reasoning, and judgment (2).

Brain structural anomalies are frequently documented in schizophrenia, with comprehensive meta-analyses identifying extensive cortical thinning and reduced cortical surface area, with the most significant effects predominantly observed in the frontal and temporal lobe regions (3). Schizophrenia is associated with abnormalities in volume (4) and shape measures (5) of subcortical structures, as well as their asymmetry (6). The ENIGMA Consortium demonstrated subcortical shape variations in individuals with schizophrenia, such as the predominance of concave, disease-related thinning, and surface contraction in the bilateral amygdala, hippocampus, accumbens, and thalamus. Also, they found a predominance of convex, disease-related shape differences in the bilateral putamen and the pallidum and a mix of concave and convex shape differences in the caudate (7). Compared to whole-structure volume approaches, shape analysis-based methods, such as the one used in this study, may reveal much subtler and more anatomically informative differences for the questioned areas by considering the complexity of the subcortical structures.

Highlights

- **FreeSurfer was used to analyze subcortical shape in schizophrenia patients.**
- **Altered surface area and thickness of subcortical structures were observed.**
- **The dose of antipsychotic medication did not significantly influence these changes.**

Correspondence Address: Ali Saffet Gönül, SoCAT Lab Department of Psychiatry, School of Medicine Ege University, Izmir, Türkiye • **E-mail:** ali.saffet.gonul@ege.edu.tr
Received Date: 25.08.2025, **Accepted Date:** 16.02.2026, **Publication Date:** 18.08.2026

In this study, we investigated the shape characteristics of seven subcortical structures (i.e., the hippocampus, amygdala, caudate, putamen, globus pallidus, nucleus accumbens, and thalamus). We compared the surface area and thickness measures of these subcortical structures between schizophrenia patients and healthy controls by processing the images using FreeSurfer and subsequently following the subcortical shape analysis protocol proposed by the ENIGMA Consortium. Unlike the ENIGMA study, which is based on data from multiple centers, the current study focuses on data from a single center (SoCAT Lab). Conducting the study in a single center allows for greater control over variables, helping to confirm that inter-site differences do not influence the results but instead reflect a genuine effect. Additionally, a single-center replication enables researchers to evaluate whether the findings apply to more specific patient populations or are relevant within a particular institution's context.

METHODS

Study Design

We included 57 patients who applied to the Psychiatry Department of Ege University School of Medicine between January 01, 2019 – December 01, 2021, and 37 healthy controls of similar age. Inclusion criterion for patients: Diagnosis of schizophrenia according to DSM-5 (Diagnostic and Statistical Manual of Mental Disorders 5th Edition, 2013). Exclusion criteria for patients and controls: 1) Any axis I disorder (except schizophrenia for patients), 2) Contraindication for MRI examination (pacemaker or claustrophobia), 3) Head trauma or neurological disease with loss of consciousness, 4) Being pregnant, 5) Any uncontrolled medical disease. Healthy controls were excluded if they had a family history of a psychotic illness. An experienced psychiatrist confirmed the diagnosis using SCID (Structured Clinical Interview for DSM Disorders, 2018) and assessed symptom severity with the Positive and Negative Syndrome Scale (PANSS) and Scale for the Assessment of Negative Symptoms (SANS) within the week prior to the magnetic resonance (MR) scan. All participants gave their written informed consent before the procedures. The Ege University Faculty of Medicine, Ethics Committee approved the study with the decision number 24-3T/89 (19-12T/42), and the guidelines of the Declaration of Helsinki (2013) were followed. Antipsychotic medications were converted to chlorpromazine (CPZ) equivalent doses to ensure a homogeneous assessment of drug effects (8).

Magnetic Resonance Imaging (MRI) Acquisition

Magnetic resonance scans were performed within the same week of clinical assessment. 3D T1-weighted, sagittal, magnetization prepared rapid gradient echo (MPRAGE) scans of the head *(repetition time (TR)/ echo time (TE)/inversion time (TI)*=1600/2.21/900 ms; *flip angle (FA)*=9; *field of view (FOV)*=256 mm*; number of excitation (Nex)=1; GRAPPA: acceleration factor=2; matrix*=246×256; 1×1×1 mm *voxels; slice thickness*=1 mm; 160 *slices)*, 2D T2 weighted axial, Turbo Spin Echo (TSE) scans of the whole brain *(TR/TE*=2500/117 ms*; FOV*=200 mm; *Nex*=1; *GRAPPA*=2; *matrix*=246×256; *slice thickness*=5 mm; *interslice gap*=1.8 mm; 0.6×0.6×5 mm *voxels*; 20 slices*)* and 3D coronal fluid attenuated inversion recovery (FLAIR) scans were acquired on a Siemens Magnetom Verio, Numaris/4, Syngo MR B17, 3T MR scanner with a twelve-channel head coil (Erlangen, Germany). Turbo spin echo and FLAIR scans were used for clinical evaluation by a neuroradiologist, and MPRAGE scans were used for the region of interest analysis. All imaging data were transferred to a PC workstation for further analysis.

Image Processing

Magnetic resonance scans were processed using FreeSurfer v7.4.1 (9–12) to obtain structural measurements. A summary of the recon-all protocol is as follows: First, the skull is stripped from the anatomical image. Then, the interface between the white and grey matter for both hemispheres is estimated and refined. This boundary is then used as a base from which the edge of the grey matter is searched. Once the edge is reached, the resulting surface, which is the pial surface, is inflated into a sphere and normalized according to a template called fsaverage. Once the surface map is normalized to this template, the Desikan-Killiany (13) and the Destrieux (14) atlases can be used to parcellate the cortex into anatomically distinct regions.

Quality assessment of the FreeSurfer outputs was conducted via SynthSeg (15,16), which is a deep learning tool for the automated analysis of brain magnetic resonance scans that also provides quality control of segmentation results without the need for retraining. All of the reconstructions passed the quality check.

To assess the shape measurements of the subcortical regions, namely the left and right thalamus, caudate, putamen, pallidum, accumbens, hippocampus, and amygdala, we followed the ENIGMA-Shape pipeline (17). A summary of the pipeline is as follows: Mesh models were produced for the boundaries of the subcortical regions. Shape curvatures and medial features were matched to a template using the Medial Demons framework (18,19). For each resulting vertices from the meshes, radial distance and the natural logarithm of the Jacobian determinant were calculated to quantify shape. The radial distance indicates how far the vertex is from the central curve of the structure, serving as a measure of its thickness. Natural logarithm of the Jacobian determinant shows the deformation needed to align the subject-specific vertex with a template, reflecting surface dilation caused by volume changes in specific regions, thereby providing a localized measurement of the structure's surface area. The quality control of the subcortical segmentations was conducted via visual inspection for any artifacts according to anatomical accuracy (20).

Statistical Analysis

Vertex-wise unilateral mass-univariate analysis was performed on R Statistical Software v4.1.2 (21) using the ENIGMA-Shape package (17). The effects of the diagnosis and the CPZ equivalent doses of antipsychotic medication administered to the schizophrenia patients on the thickness and the surface area were tested using linear models, with sex, age, age centered squared, interaction of age squared centered and sex, interaction of age centered and sex, intracranial volumes (ICV) accounted for linearly as covariates. Regression coefficients (β) and p-values for both group and CPZ analyses, and Cohen's d effect sizes (22) for group analysis were calculated. P-values were corrected for multiple comparisons using a modified searchlight false discovery rate (FDR) procedure, accounting for spatial dependency between neighboring vertices, and applied globally across all structures and measures within each model (23,24).

RESULTS

Sample Characteristics

Patient demographic data and other descriptive information are included in Table 1.

Group Differences

3.2.1. Shape surface area

Compared with healthy controls, schizophrenia patients showed lower surface area in the left hippocampus (Cohen's d=−0.72; 4.41% of vertices), right thalamus (d=−0.68; 33.75%), left thalamus (d=−0.80; 57.23%), right amygdala (d=−0.76; 13.40%), right accumbens (d=−0.76; 44.67%), and left accumbens (d=−0.62; 21.58%). Regions demonstrating higher surface area

Table 1. Clinical and demographic variables of patient and control groups

Demographic and clinical data	Patients (N=57)	Control group (N=37)	Comparison
Sex distribution (male %)	46 (80.7%)	14 (37.8%)	X^2 =16, p <0.001*
Mean age (± SD)	34.4 ± 8.3	33.9 (±7.7)	W=1017, p >0.05**
Antipsychotic chlorpromazine equivalent dose (mg/day)	97.5–2735; mean=746.37 ± 552.7	-	-
PANSS positive subscale score (± SD)	12 (±5.7)	-	-
PANSS total score (± SD)	62 (±14.7)	-	-
SANS score (± SD)	39.4 (±20.1)	-	-

SD: standard deviation; PANSS: positive and negative syndrome scale; SANS: scale for the assessment of negative symptoms; *: Chi-squared test; **: Wilcoxon rank sum test.

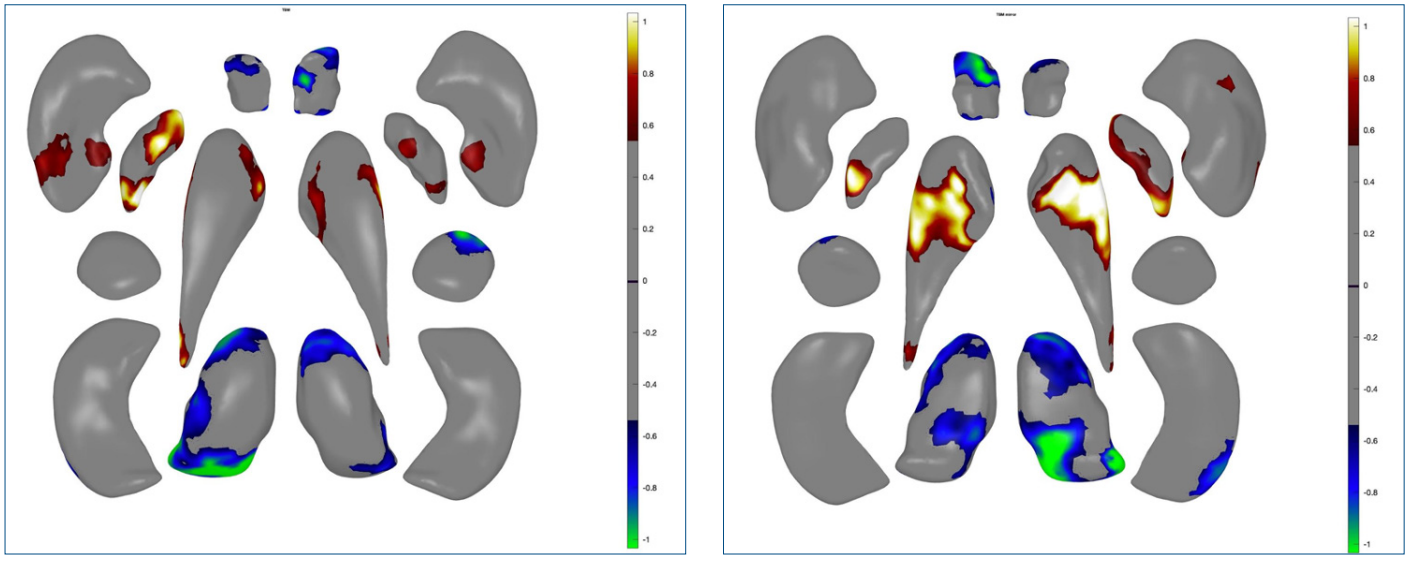

A B

Figure 1. Vertex-wise effects of diagnosis (i.e., schizophrenia vs. control) on each hemisphere for surface dilation/contraction (log Jacobian determinant), with a color scale that indicates the intensity of Cohen's d effect sizes. Cooler colors (i.e., negative effect sizes) indicate surface contraction for schizophrenia as compared to controls, and warmer colors (i.e., positive effect sizes) indicate surface dilation, with grey color indicating nonsignificant surface vertices after multiple comparisons correction. (A) Tensor based morphometry (TBM). (B) TBM mirrored.

included the right putamen (d=0.64; 1.80%), left putamen (d=0.62; 8.58%), left caudate (d=0.86; 27.61%), right pallidum (d=0.72; 16.36%), and left pallidum (d=0.77; 54.57%). The right caudate demonstrated both higher and lower surface area (d=0.78 and −0.66; 28.21%). No significant surface area effects were observed in the right hippocampus or left amygdala. Vertex-wise effects of diagnosis for surface area are provided in Figure 1.

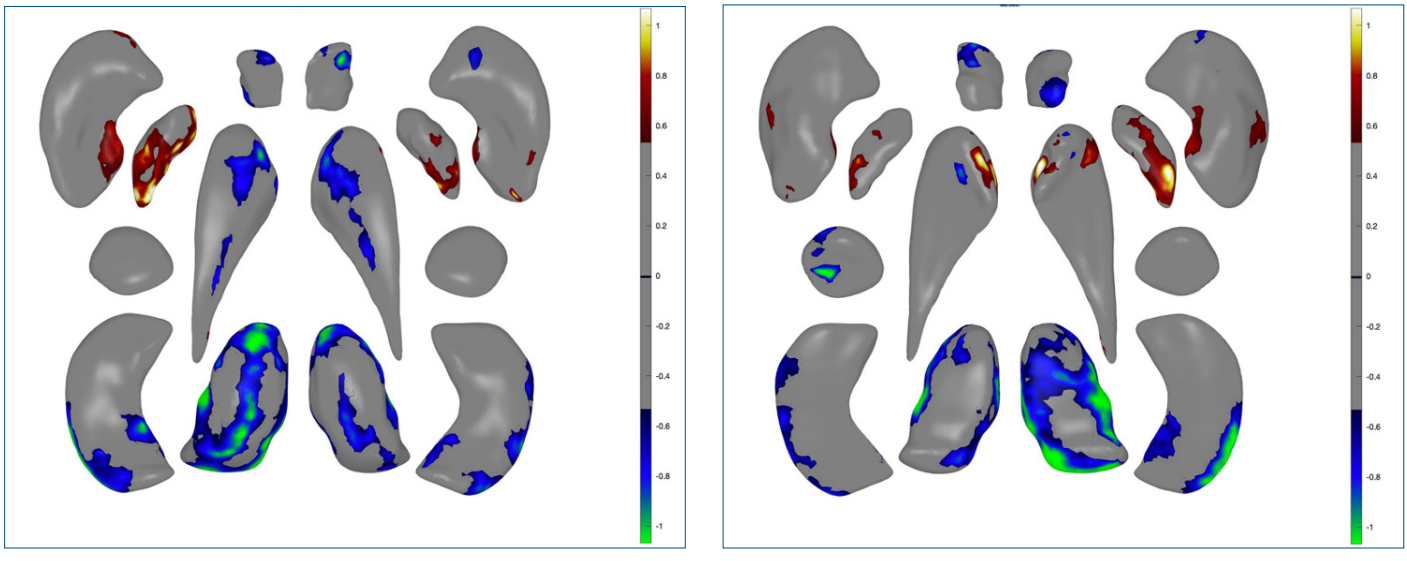

A B

Figure 2. Vertex-wise effects of diagnosis (i.e., schizophrenia vs. control) on each hemisphere for thickness, with a color scale that indicates the intensity of Cohen's d effect sizes. Cooler colors (i.e., negative effect sizes) indicate thinning for schizophrenia as compared to controls, and warmer colors (i.e., positive effect sizes) indicate thickening, with grey color indicating nonsignificant surface vertices after multiple comparisons correction. (A) Radial distance (RAD). (B) RAD mirrored.

Shape thickness

Schizophrenia patients (n=57) showed lower thickness in the right hippocampus (Cohen's d=-0.67; 19.15% of vertices), left hippocampus (d=−0.76; 20.12%), right thalamus (d=-0.72; 42.40%), left thalamus (d=-0.81; 71.78%), right amygdala (d=−0.73; 9.19%), right accumbens (d=-0.71; 17.16%), and left accumbens (d=-0.66; 25.28%). The right pallidum demonstrated higher thickness (d=0.68; 21.19%). Regions demonstrating both higher and lower thickness included the right putamen (d=0.65 and -0.66; 4.53%), left putamen (d=0.65 and -0.69; 10.34%), right caudate (d=0.76 and -0.69; 14.92%), left caudate (d=0.74 and -0.70; 14.97%), and left pallidum (d=0.74 and -0.56; 58.57%). No significant thickness effects were detected in the left amygdala. Vertex-wise effects of diagnosis for thickness are provided in Figure 2.

Antipsychotic Effect

Vertex-wise linear models estimating β coefficients for the association between antipsychotic dose and subcortical shape measures revealed no vertices that remained significant after multiple comparisons correction.

DISCUSSION

In this single-center study, we used the ENIGMA-Shape pipeline to characterize vertex-wise subcortical morphometry differences between individuals with schizophrenia and healthy controls, adjusting for ICV and nonlinear age and sex interaction terms in our linear models. Overall, our findings converge with prior multi-center ENIGMA work by demonstrating a predominance of surface contraction and thinning in limbic and thalamic structures in schizophrenia, alongside surface expansion and/or thickening in parts of the basal ganglia. Specifically, schizophrenia patients showed reduced surface area in the left hippocampus, bilateral thalamus, bilateral nucleus accumbens, and the right amygdala, while surface area increases were observed in the bilateral putamen, left caudate, and bilateral pallidum. For thickness, patients exhibited widespread thinning in the bilateral hippocampus, bilateral thalamus, and bilateral accumbens, as well as the right amygdala, with thickening most clearly observed in the right pallidum. Importantly, several structures -particularly the caudate and putamen, and to a lesser extent the left pallidum- showed bidirectional patterns (co-occurring regions of both increases and decreases), underscoring that schizophrenia-related morphometric alterations are spatially heterogeneous within individual nuclei rather than uniformly expressed across an entire structure.

Our results are broadly consistent with large-scale volumetric ENIGMA analyses. Van Erp et al. (2016) (4) reported smaller hippocampus, amygdala, thalamus, and nucleus accumbens, and larger pallidum, with less consistent findings for the caudate and putamen. Our vertex-wise shape results parallel these volumetric patterns but provide additional spatial specificity, indicating that basal ganglia structures may exhibit mixed, regionally-specific expansions and contractions that could cancel out at the whole-structure volume level. This is particularly relevant for the caudate and putamen, where we observed bidirectional thickness effects and, for the right caudate, bidirectional surface area effects. Such heterogeneity may help explain why some prior volume studies report null or inconsistent findings for these nuclei despite the presence of localized abnormalities.

The findings on thickness and surface area also align with the ENIGMA-Shape meta-analysis by Gutman et al. (2021) (7), which described predominant thinning and contraction in the hippocampus, thalamus, accumbens, and amygdala, and predominant thickening/expansion in the putamen and pallidum, with mixed effects in the caudate. In our sample, the thalamus showed the broadest spatial extent of abnormality (across both thickness and surface area), consistent with the thalamus being a key hub in cortico-striato-thalamo-cortical circuitry implicated in schizophrenia (7). At the same time, our results suggest some laterality differences in this cohort -most notably no significant effects in the left amygdala, and a hippocampal pattern in which thinning was bilateral, while surface contraction was more evident on the left.

Testing continuous CPZ equivalent dose within the schizophrenia group using vertex-wise linear models (β estimates) with the same covariate structure revealed that no vertices survived multiple comparisons correction for associations between CPZ equivalent dose and either thickness or surface area. This null finding should be interpreted cautiously. First, current CPZ equivalent dose may not adequately capture cumulative exposure, medication history, adherence, or antipsychotic class effects. Second, antipsychotic dose is subject to confounding by indication, where higher doses may index more severe illness or treatment resistance rather than being a direct driver of morphometric differences. Finally, our sample size limits power to detect subtle dose-related effects that may be detectable in very large cohorts. Notably, Gutman et al. (2021) (7) reported small but significant medication-related associations in their large meta-analysis; differences in sample size, heterogeneity, and statistical power may therefore account for the discrepancy. Longitudinal designs with detailed medication exposure metrics (e.g., cumulative dose, duration, class, polypharmacy, and treatment changes) will be important for clarifying whether and how antipsychotic exposure relates to subcortical shape.

It is also important to consider the differences in effect sizes between our study and those in Gutman et al. (2021) (7). Larger effect sizes observed in our study could be attributed to the higher sampling variability due to relatively smaller sample size or increased clinical severity among patients from our single center compared to the patient populations in the meta-analysis. Marek et al. (2022) (25) demonstrated that effect sizes can be inflated in small sample sizes due to higher sampling variability. However, in our study population, which constitutes data from a tertiary university hospital that represents the burden of the disease from that region sufficiently, there exists higher clinical severity which can be observed through SANS scores and antipsychotic doses (Table 1). This may serve as a potential indicator for the difference in effect sizes between our underrepresented study population and the larger meta-analysis, rather than random inflation, as higher clinical severity was demonstrated to be correlated with the progression of the disease in terms of morphological changes (7). Future work in larger and more diverse samples -especially those that better represent clinically severe subgroups- will be necessary to determine whether stronger localized effects reflect true clinical enrichment versus sampling variability.

The predominance of concordant thinning and surface contraction across limbic structures (hippocampus, amygdala, nucleus accumbens) and the thalamus suggests a potential structural basis for core symptom domains in schizophrenia, given their roles in memory, emotion regulation, and reward-guided behavior (2,4). Inward deformation within this circuitry may be associated with cognitive inefficiency and emotional and motivational disturbances that contribute to functional impairment. Large ENIGMA studies have shown that these same subcortical regions are consistently smaller at the whole-structure level (4) and demonstrate a meta-analytic predominance of concave, disease-related thinning and contraction patterns (7), supporting the view that vertex-wise inward deformation may be a sensitive marker of clinically meaningful network compromise. Although longitudinal and symptom-linked analyses are needed, our findings encourage future work to test whether limbic inward deformation tracks dimensional outcomes in affect, cognition, and memory, and whether it can help stratify patients for interventions aimed at improving cognitive and functional outcomes (2,7).

From a neurobiological perspective, the pattern of thinning and contraction in the thalamus and nucleus accumbens is consistent with postmortem reports of reduced cellular elements in these regions (26). Pakkenberg (1990) (26) reported reduced numbers of neurons and glial cells in the mediodorsal thalamic nucleus and nucleus accumbens in schizophrenia, with less clear differences in the ventral pallidum and basolateral nucleus of the amygdala. In our data, the thalamus and accumbens showed robust and spatially extensive reductions, which may be compatible with cellular-level reductions and/or altered neuropil. In contrast, the pallidum showed surface expansion bilaterally and thickening on the right, suggesting that pallidal abnormalities may reflect different mechanisms (e.g., altered connectivity, tissue composition, or medication- and illness-related neuroplasticity), and emphasizing the need for studies that bridge MRI-derived morphometry with cellular and molecular measures.

Within the medial temporal lobe, schizophrenia-related abnormalities in the hippocampus have been linked to interneuron and synaptic pathology (27). While Schmitt et al. (2009) (27) did not find group differences in total neuron number or astrocyte density in the hippocampus, other work suggests deficits in interneuron density in hippocampal formation, particularly in male patients (28). In our cohort (predominantly male), the hippocampus showed consistent thinning bilaterally, which may relate to alterations in interneuron populations and/or microcircuit organization that may not be detectable by gross neuron counts alone. The amygdala findings in our sample were more lateralized, with significant thinning and contraction in the right amygdala but not the left. Kreczmanski et al. (2007) (29) reported reduced neuron number in the lateral nucleus of the amygdala and putamen, and reduced total neuron number in the caudate. Our observation of localized abnormalities and bidirectional patterns in the caudate and putamen is compatible with the idea that multiple, potentially competing processes (neurodevelopmental alterations, compensatory remodeling, and/or treatment- or illness-related plasticity) may contribute to heterogeneous shape effects within basal ganglia structures.

Several limitations should be noted. The study is cross-sectional and single-center, which restricts causal inference and may limit generalizability. Clinical and treatment variables are complex and may be incompletely captured by a single current-dose measure. Nonetheless, a key strength of this work is its implementation of an ENIGMA-consistent modeling strategy -including ICV, and nonlinear age and sex interaction terms- and its contribution of data from Türkiye, an often underrepresented population in large neuroimaging consortia. Replication in larger regional samples and inclusion in future meta-analytic efforts will help clarify the reproducibility and clinical relevance of these spatially specific shape alterations.

As a result, the findings from this study align with those of the larger ENIGMA investigation of subcortical structures in schizophrenia, emphasizing the value of vertex-wise shape analysis for revealing anatomically specific alterations that may be obscured in volume-based approaches. Rather than random inflation, the higher observed effect sizes may be attributable to the relatively greater baseline clinical severity of our study population with a relatively smaller but moderate sample size, which is also an often-underrepresented population in broader consortia. This study not just validates the results of the meta-analysis, but also paves the way for clinically more severe subgroups of populations that are underrepresented to be integrated in larger studies. These results underscore the importance of considering the clinical characteristics of the study sample when interpreting neuroanatomical alterations, as they can significantly influence effect sizes and the overall interpretation of brain changes in schizophrenia.

Acknowledgements: *This study was presented in the research paper award competition at the 60th Turkish National Psychiatry Congress (November 3, 2024, Antalya) and received first prize. We would also like to thank Paul Thompson for his valuable input on our study.*

Ethics Committee Approval: All procedures performed in studies involving human participants were in accordance with the ethical standards of the institutional national research committee [The Research Ethics Committee at The Ege University Faculty of Medicine, 24-3T/89 (19-12T/42)] and with the 2013 World Medical Association Declaration of Helsinki (2013).

Informed Consent: All participants gave their written informed consent before the procedures.

Peer-review: Externally peer-reviewed.

Author Contributions: Concept- ASG; Design- SÖ, BT, ÇK, YA, ACH, FY, ASG; Supervision- ASG; Resource- ASG; Materials- ACH, FY, YE, ASG; Data Collection and/or Processing- ACH, FY, YE, ASG; Analysis and/or Interpretation- SÖ, BT, ÇK, YA; Literature Search- SÖ, BT, ÇK, YA, FY, ASG; Writing- SÖ, BT, ÇK, YA, FY, ASG; Critical Reviews- ASG.

*These authors contributed equally to this work and share first authorship.

Conflict of Interest: The authors declared that there is no conflict of interest.

Financial Disclosure: This study was funded by Ege University Research Foundation with the grant number TTU-2019-20974.

During the preparation of this work, the authors used GPT4 (OpenAI) in order to increase readability and check spelling and grammar. After using this tool/service, the authors reviewed and edited the content as needed and take full responsibility for the content of the publication.

REFERENCES

1. Charlson FJ, Ferrari AJ, Santomauro DF, Diminic S, Stockings E, Scott JG, et al. Global epidemiology and burden of schizophrenia: findings from the Global Burden of Disease Study 2016. Schizophr Bull. 2018;44:1195–1203. [Crossref]
2. Owen MJ, Sawa A, Mortensen PB. Schizophrenia. Lancet. 2016;388:86–97. [Crossref]
3. Van Erp TGM, Walton E, Hibar DP, Schmaal L, Jiang W, Glahn DC, et al. Cortical brain abnormalities in 4474 individuals with schizophrenia and 5098 control subjects via the Enhancing Neuro Imaging Genetics Through Meta Analysis (ENIGMA) consortium. Biol Psychiatry. 2018;84:644–654. [Crossref]
4. Van Erp TGM, Hibar DP, Rasmussen JM, Glahn DC, Pearlson GD, Andreassen OA, et al. Subcortical brain volume abnormalities in 2028 individuals with schizophrenia and 2540 healthy controls via the ENIGMA consortium. Mol Psychiatry. 2016;21:547–553. [Crossref]
5. Mamah D, Wang L, Barch D, De Erausquin GA, Gado M, Csernansky JG. Structural analysis of the basal ganglia in schizophrenia. Schizophr Res. 2007;89:59–71. [Crossref]
6. Okada N, Fukunaga M, Yamashita F, Koshiyama D, Yamamori H, Ohi K, et al. Abnormal asymmetries in subcortical brain volume in schizophrenia. Mol Psychiatry. 2016;21:1460–1466. [Crossref]
7. Gutman BA, Van Erp TG, Alpert K, Ching CRK, Isaev D, Ragothaman A, et al. A meta-analysis of deep brain structural shape and asymmetry abnormalities in 2,833 individuals with schizophrenia compared with 3,929 healthy volunteers via the ENIGMA Consortium. Hum Brain Mapp. 2022;43:352–372. [Crossref]
8. Leucht S, Samara M, Heres S, Davis JM. Dose equivalents for antipsychotic drugs: the DDD method. Schizophr Bull. 2016;42 Suppl 1:S90–S94. [Crossref]
9. FreeSurfer. FreeSurfer software suite [Internet]. [cited 2025 Aug 24]. Available from: https://surfer.nmr.mgh.harvard.edu/
10. Dale AM, Fischl B, Sereno MI. Cortical surface-based analysis. I. Segmentation and surface reconstruction. Neuroimage. 1999;9:179–194. [Crossref]
11. Fischl B, Salat DH, Busa E, Albert M, Dieterich M, Haselgrove C, et al. Whole brain segmentation: automated labeling of neuroanatomical structures in the human brain. Neuron. 2002;33:341–355. [Crossref]
12. Fischl B, Van Der Kouwe A, Destrieux C, Halgren E, Ségonne F, Salat DH, et al. Automatically parcellating the human cerebral cortex. Cereb Cortex. 2004;14:11–22. [Crossref]
13. Desikan RS, Ségonne F, Fischl B, Quinn BT, Dickerson BC, Blacker D, et al. An automated labeling system for subdividing the human cerebral cortex on MRI scans into gyral-based regions of interest. Neuroimage. 2006;31:968–980. [Crossref]

14. Destrieux C, Fischl B, Dale A, Halgren E. Automatic parcellation of human cortical gyri and sulci using standard anatomical nomenclature. Neuroimage. 2010;53:1–15. [Crossref]
15. Billot B, Greve DN, Puonti O, Thielscher A, Van Leemput K, Fischl B, et al. SynthSeg: segmentation of brain MRI scans of any contrast and resolution without retraining. Med Image Anal. 2023;86:102789. [Crossref]
16. Billot B, Magdamo C, Cheng Y, Arnold SE, Das S, Iglesias JE. Robust machine learning segmentation for large-scale analysis of heterogeneous clinical brain MRI datasets. Proc Natl Acad Sci U S A. 2023;120:e2216399120. [Crossref]
17. ENIGMA. ENIGMA-Shape Analysis [Internet]. [cited 2025 Aug 24]. Available from: https://enigma.usc.edu/ongoing/enigma-shape-analysis/
18. Gutman BA, Hua X, Rajagopalan P, Chou Y-Y, Wang Y, Yanovsky I, et al. Maximizing power to track Alzheimer's disease and MCI progression by LDA-based weighting of longitudinal ventricular surface features. Neuroimage. 2013;70:386–401. [Crossref]
19. Gutman BA, Madsen SK, Toga AW, Thompson PM. A family of fast spherical registration algorithms for cortical shapes. In: Shen L, Liu T, Yap PT, Huang H, Shen D, Westin CF, editors. Multimodal Brain Image Analysis. MBIA 2013. Lecture Notes in Computer Science, vol 8159. Springer, Cham. (pp. 246–257). [Crossref]
20. ENIGMA Cortical Quality Control Protocol 2.0 (April 2017). [cited 2025 Aug 24]. Available from: https://enigma.ini.usc.edu/protocols/imaging-protocols/
21. R Core Team. The R Project for Statistical Computing. 2021 [cited 2025 Aug 24]. Available from: https://www.R-project.org/
22. Cohen J. A power primer. Psychol Bull. 1992;112:155–159. [Crossref]
23. Kriegeskorte N, Goebel R, Bandettini P. Information-based functional brain mapping. Proc Natl Acad Sci U S A. 2006;103:3863–3868. [Crossref]
24. Langers DR, Jansen JF, Backes WH. Enhanced signal detection in neuroimaging by means of regional control of the global false discovery rate. Neuroimage. 2007;38:43–56. [Crossref]
25. Marek S, Tervo-Clemmens B, Calabro FJ, Montez DF, Kay BP, Hatoum AS, et al. Reproducible brain-wide association studies require thousands of individuals. Nature. 2022;603:654–660. [Crossref]
26. Pakkenberg B. Pronounced reduction of total neuron number in mediodorsal thalamic nucleus and nucleus accumbens in schizophrenics. Arch Gen Psychiatry. 1990;47:1023–1028. [Crossref]
27. Schmitt A, Steyskal C, Bernstein H-G, Schneider-Axmann T, Parlapani E, Schaeffer EL, et al. Stereologic investigation of the posterior part of the hippocampus in schizophrenia. Acta Neuropathol. 2009;117:395–407. [Crossref]
28. Zhang ZJ, Reynolds GP. A selective decrease in the relative density of parvalbumin-immunoreactive neurons in the hippocampus in schizophrenia. Schizophr Res. 2002;55:1–10. [Crossref]
29. Kreczmanski P, Heinsen H, Mantua V, Woltersdorf F, Masson T, Ulfig N, et al. Volume, neuron density and total neuron number in five subcortical regions in schizophrenia. Brain. 2007;130:678–692. [Crossref]